Supporting Information for

Monocarboxylic acid etching strategy: Modulation of chemical environment of Ni nanoparticles in defective Ce-UiO-66 to construct heterogeneous interfaces for dicyclopentadiene hydrogenation

Fajie Hu, Danfeng Zhao, Rushuo Li, Yunqi Zhang, Tianyu Zhang, Xiubing Huang*, Ge Wang*

Beijing Advanced Innovation Center for Materials Genome Engineering, Beijing Key Laboratory of Function Materials for Molecule & Structure Construction, School of Materials Science and Engineering, University of Science and Technology Beijing, Beijing 100083, China

*Corresponding authors: xiubinghuang@ustb.edu.cn (X. Huang), gewang@ustb.edu.cn (G. Wang)

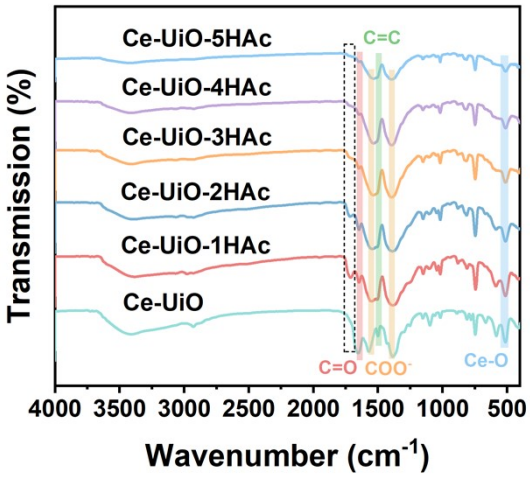

Figure S1. FTIR spectra of Ce-UiO, Ce-UiO-1HAc, Ce-UiO-2HAc, Ce-UiO-3HAc, Ce-UiO-4HAc and Ce-UiO-5HAc.

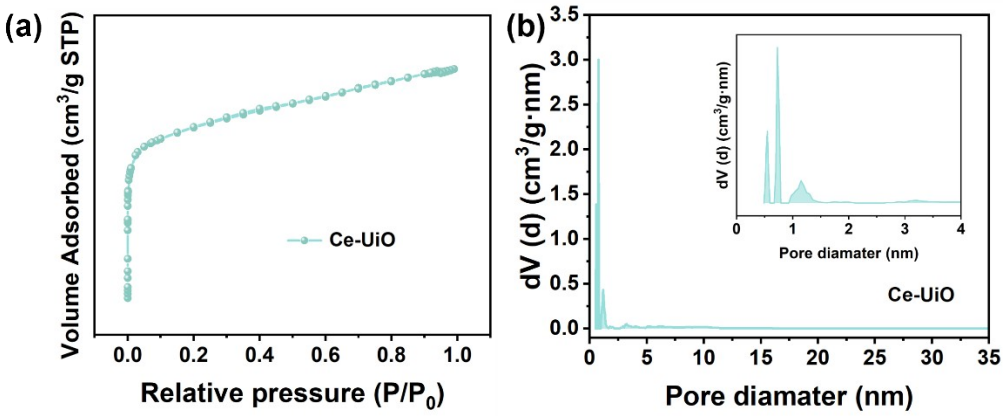

Figure S2. (a) Nitrogen adsorption isotherms and (b) pore size distributions of Ce-UiO.

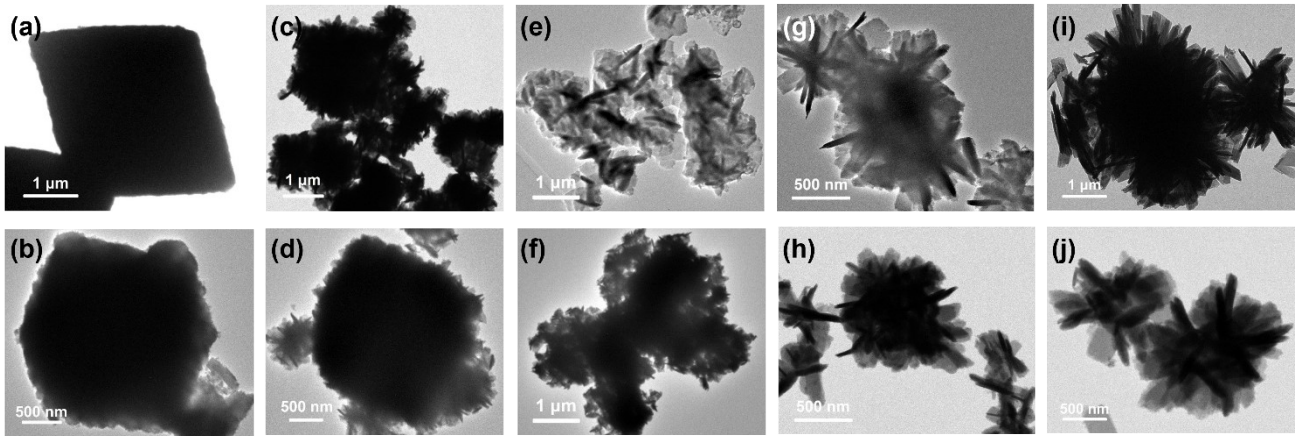

Figure S3. TEM images of (a) and (b) Ce-UiO-1HAc, (c) and (d) Ce-UiO-2HAc, (e) and (f) Ce-UiO-3HAc, (g) and (h) Ce-UiO-4HAc, (i) and (j) Ce-UiO-5HAc.

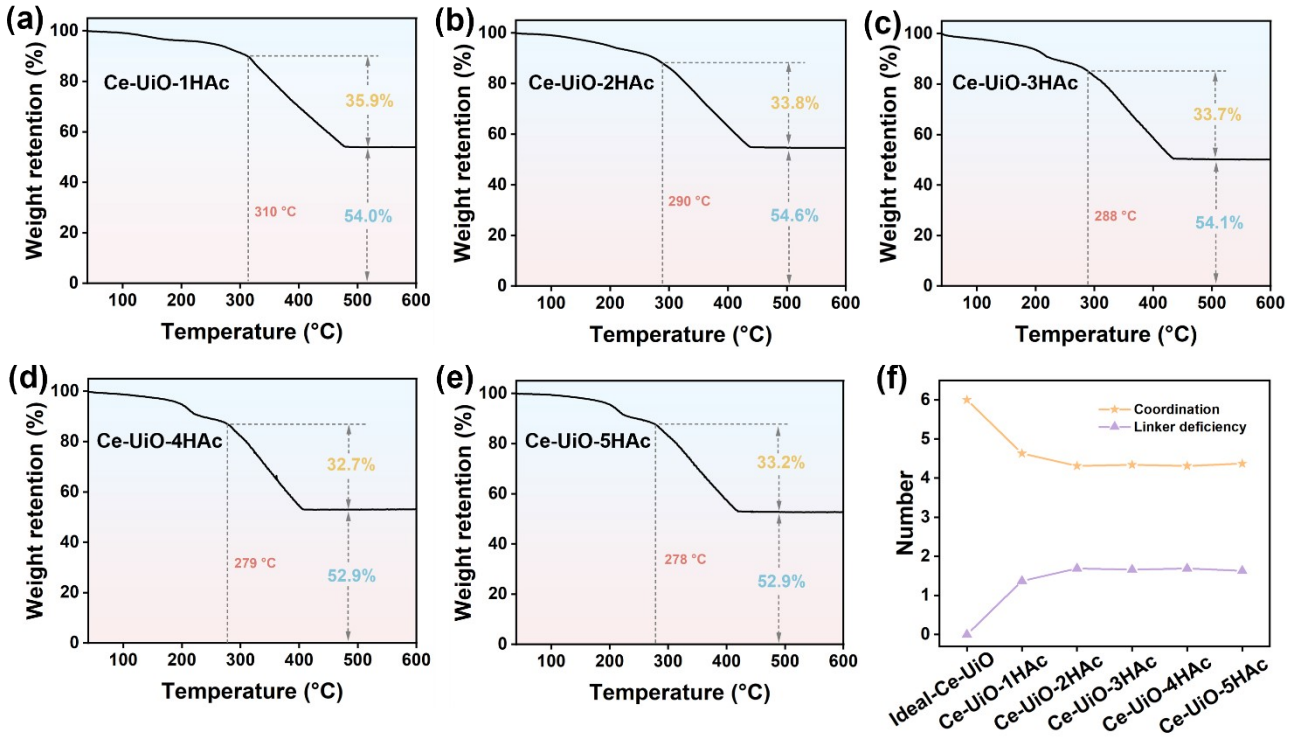

Figure S4. TG curves of (a) Ce-UiO-1HAc, (b) Ce-UiO-2HAc, (c) Ce-UiO-3HAc, (d) Ce-UiO-4HAc, (e) Ce-UiO-5HAc. (f) Number of ligand coordination and deficiency per Ce_6 cluster.

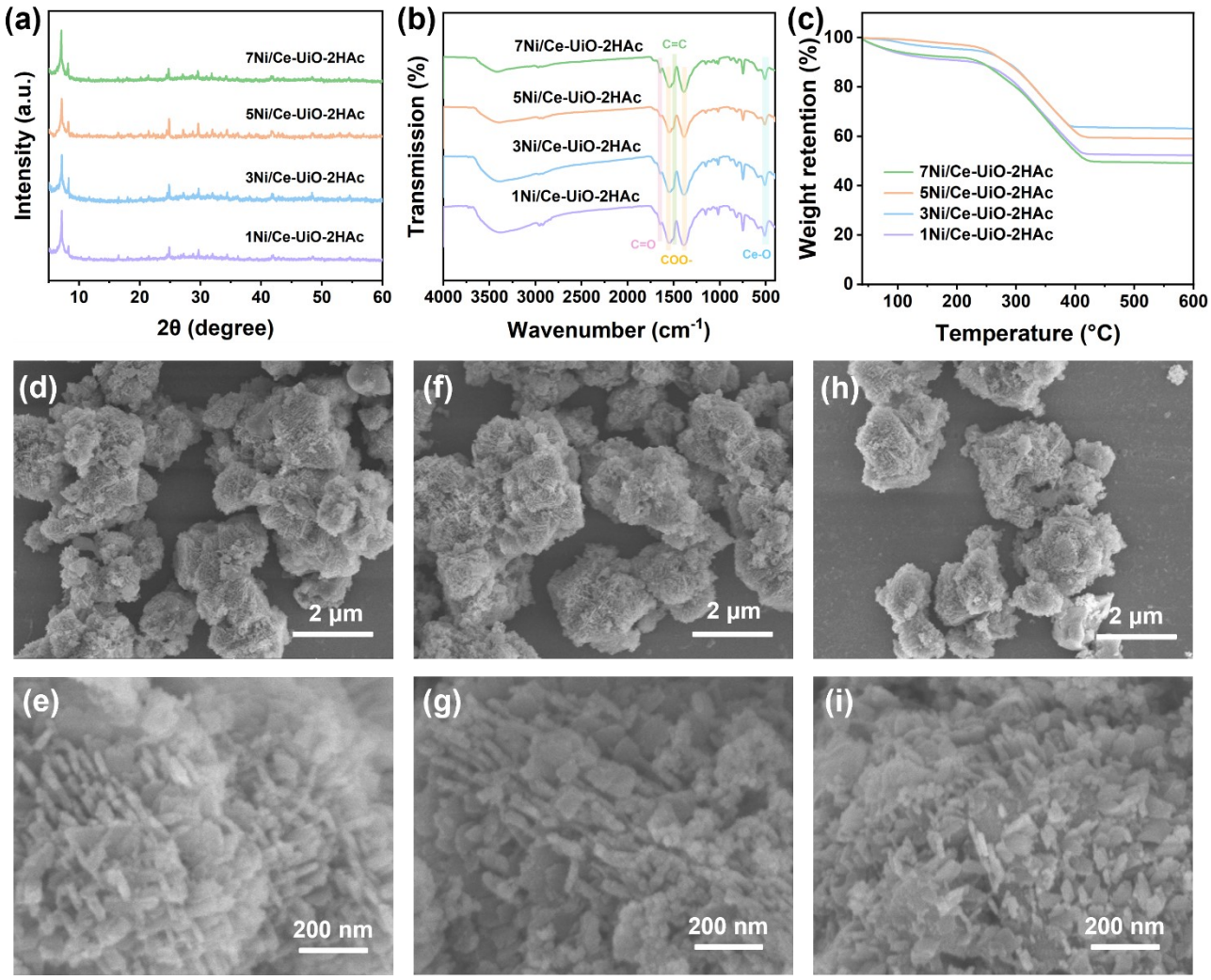

Figure S5. (a) XRD patterns, (b) FTIR spectra, (c) TG curves of 1Ni/Ce-UiO-2HAc, 3Ni/Ce-UiO-2HAc, 5Ni/Ce-UiO-2HAc, 7Ni/Ce-UiO-2HAc. SEM images of (d) and (e) 1Ni/Ce-UiO-2HAc, (f) and (g) 3Ni/Ce-UiO-2HAc, (h) and (i) 7Ni/Ce-UiO-2HAc.

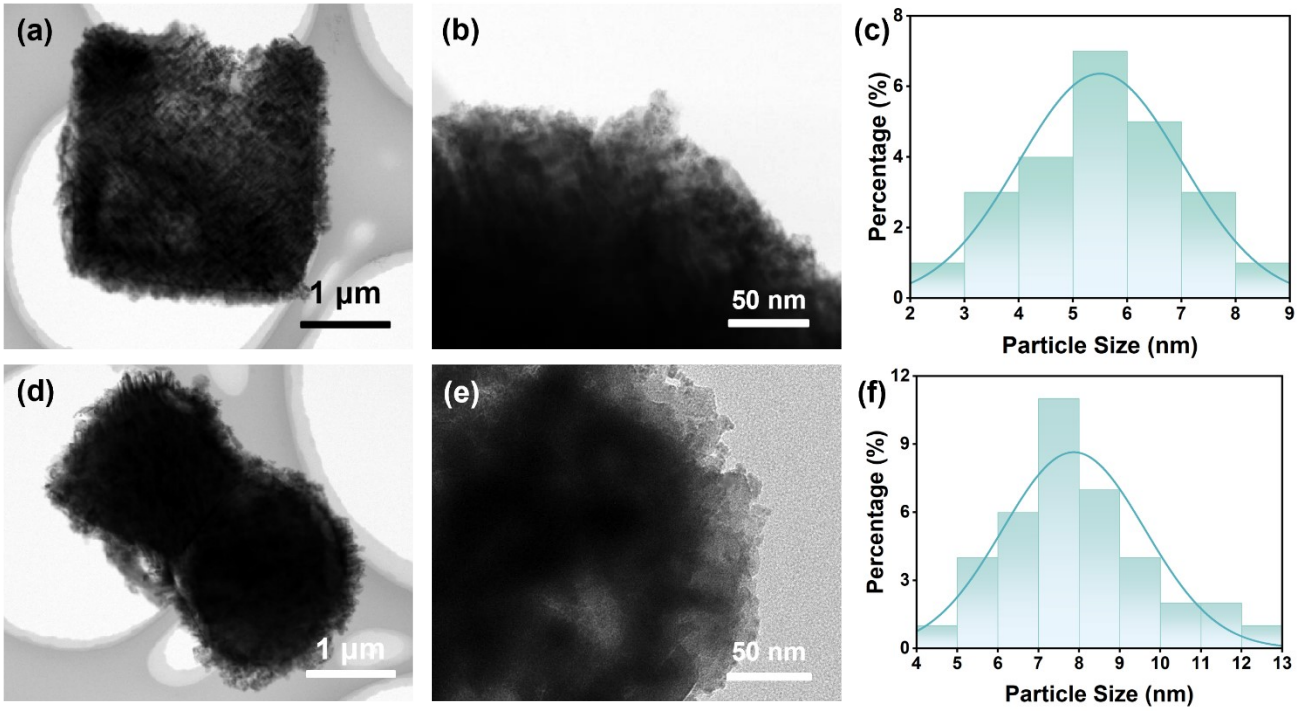

Figure S6. (a) and (b) TEM images and (c) Ni NPs size distribution of 3Ni/Ce-UiO-2HAc. (d) and (e) TEM images and (f) Ni NPs size distribution of 7Ni/Ce-UiO-2HAc.

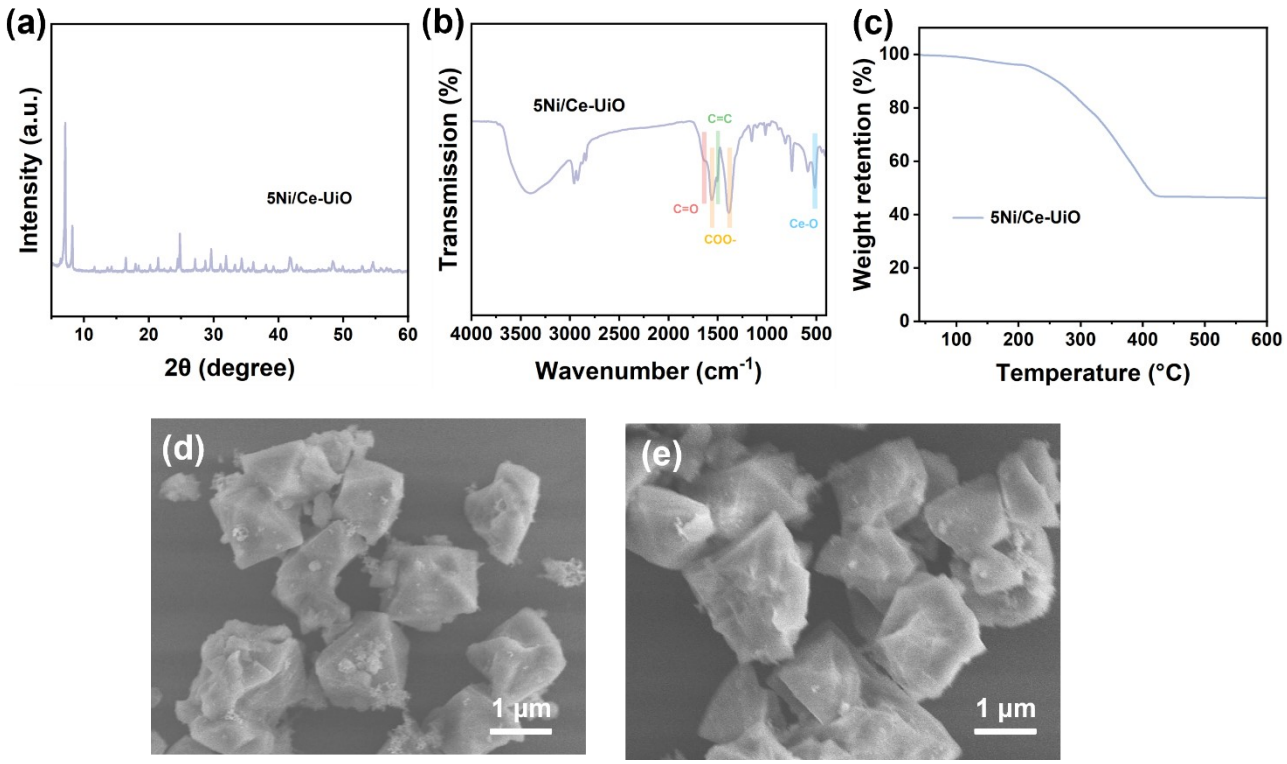

Figure S7. (a) XRD pattern, (b) FTIR spectrum, (c) TG curve, (d) and (e) SEM images of 5Ni/Ce-UiO.

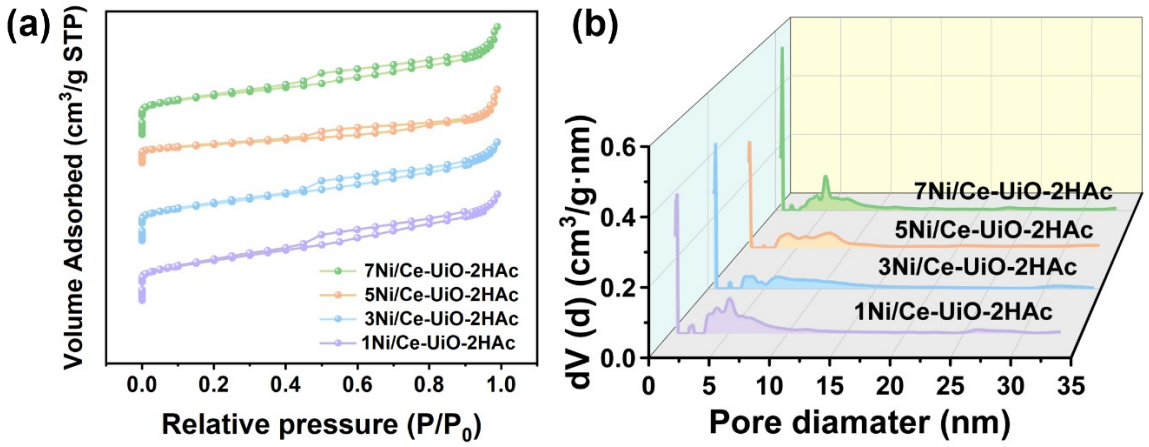

Figure S8. (a) Nitrogen adsorption isotherms and (b) pore size distributions of 1Ni/Ce-UiO-2HAc, 3Ni/Ce-UiO-2HAc, 5Ni/Ce-UiO-2HAc, 7Ni/Ce-UiO-2HAc.

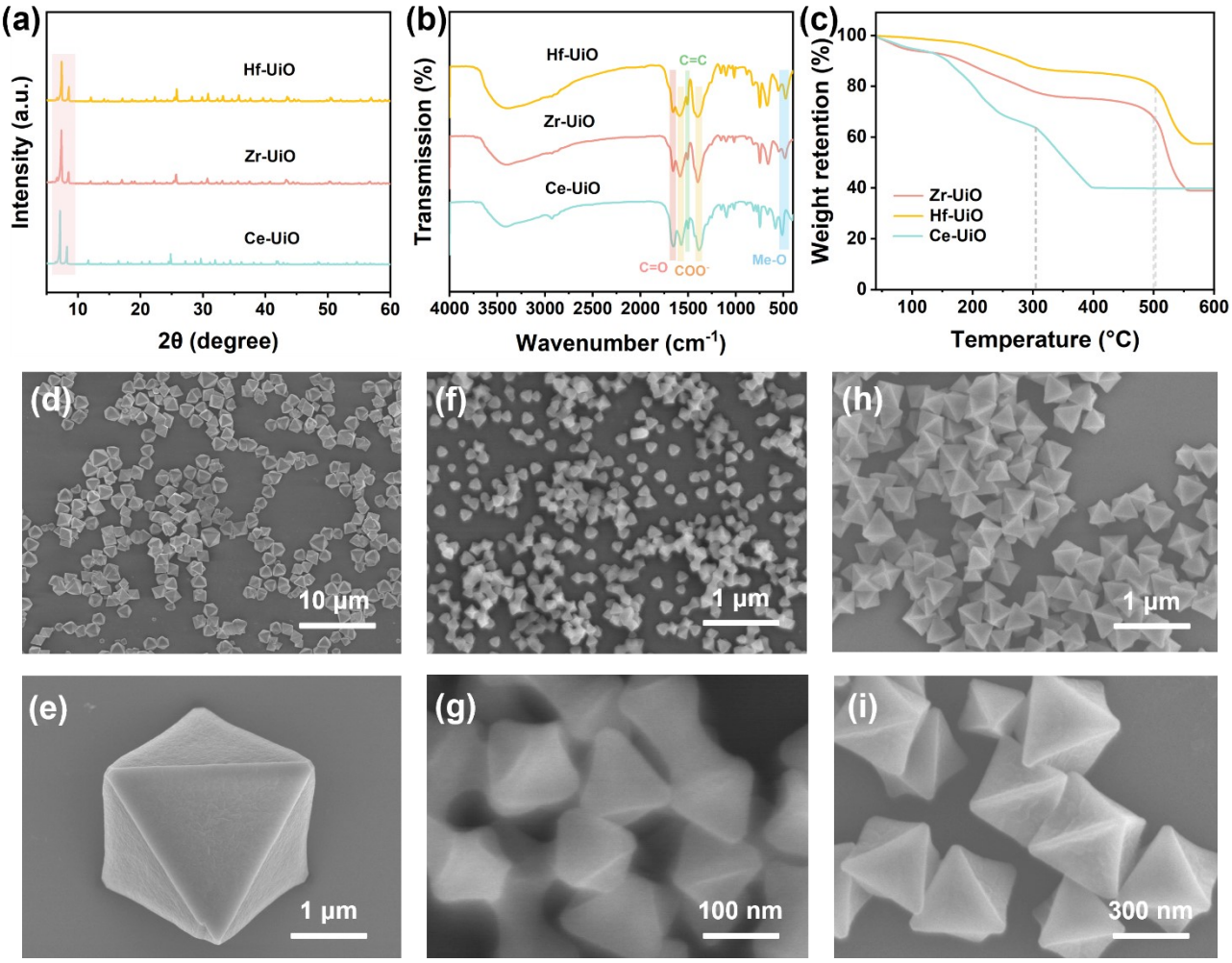

Figure S9. (a) XRD patterns, (b) FTIR spectra, (c) TG curves of Ce-UiO, Zr-UiO, Hf-UiO. SEM images of (d) and (e) Ce-UiO, (f) and (g) Zr-UiO, (h) and (i) Hf-UiO.

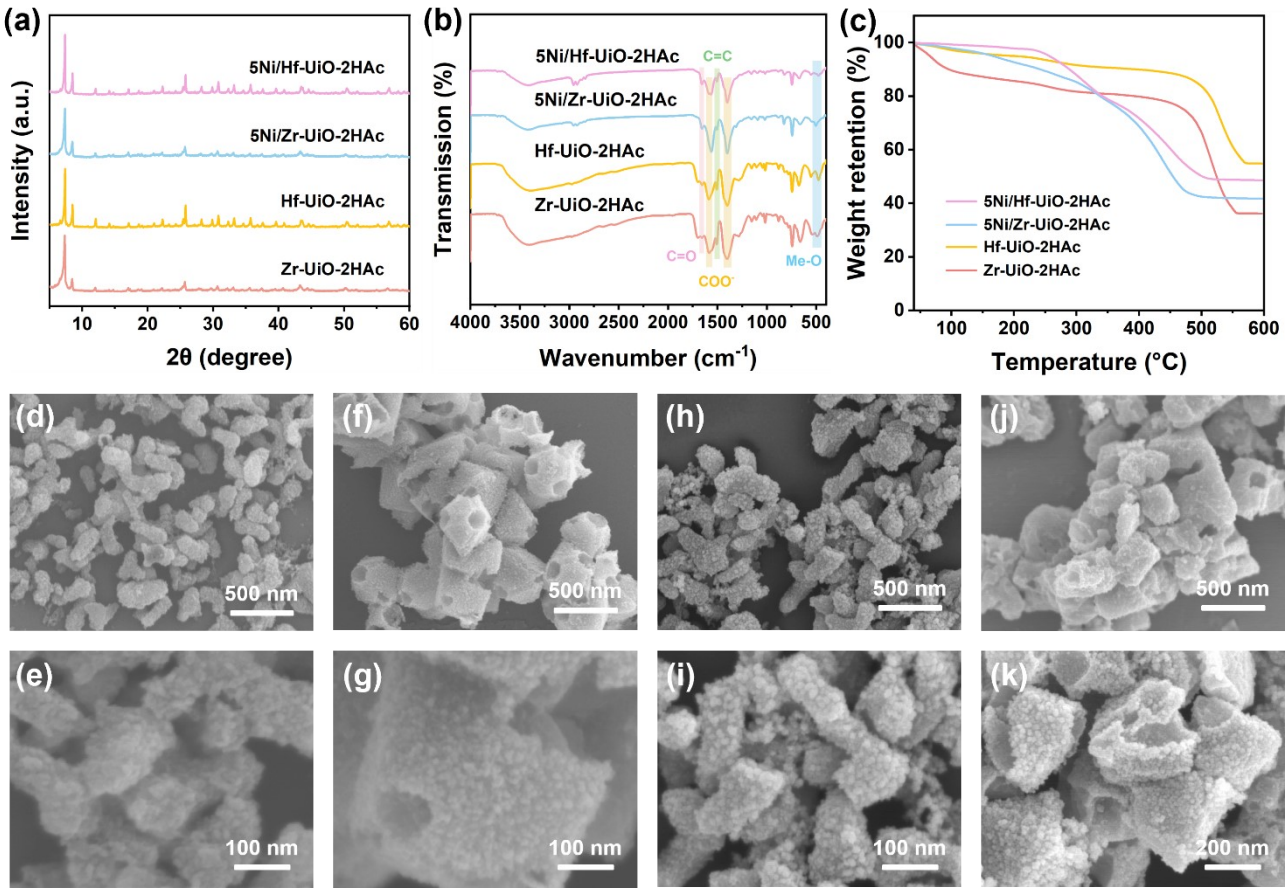

Figure S10. (a) XRD patterns, (b) FTIR spectra, (c) TG curves of Zr-UiO-2HAc, Hf-UiO-2HAc, 5Ni/Zr-UiO-2HAc, 5Ni/Hf-UiO-2HAc. SEM images of (d) and (e) Zr-UiO-2HAc, (f) and (g) Hf-UiO-2HAc, (h) and (i) 5Ni/Zr-UiO-2HAc, (j) and (k) 5Ni/Hf-UiO-2HAc.

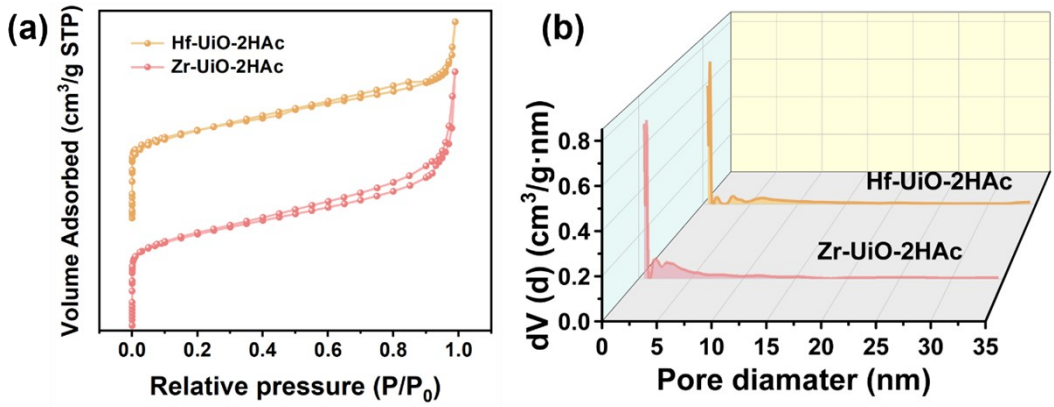

Figure S11. (a) Nitrogen adsorption isotherms and (b) pore size distributions of Zr-UiO-2HAc and Hf-UiO-2HAc.

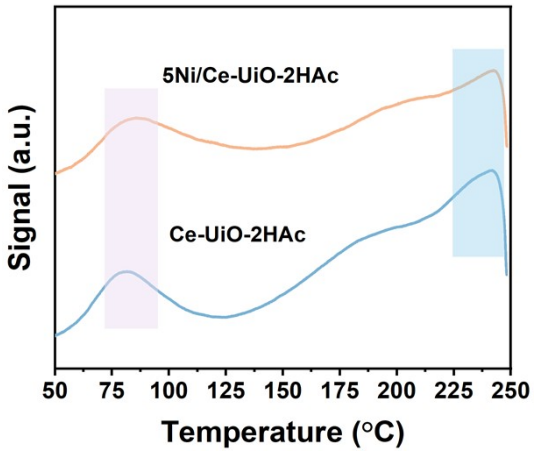

Figure S12. NH_3-TPD profiles of Ce-UiO-2HAc and 5Ni/Ce-UiO-2HAc.

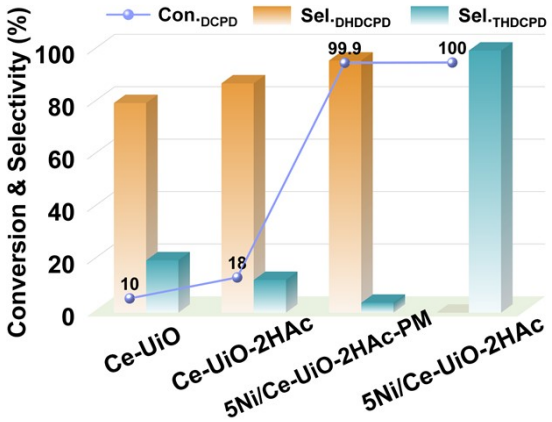

Figure S13. Conversion and selectivity (conditions: 100 ℃, 2Mpa, 60 min) for (b) Ce-UiO, Ce-UiO-2HAc, 5Ni/Ce-UiO-2Hac-PM and 5Ni/Ce-UiO-2HAc.

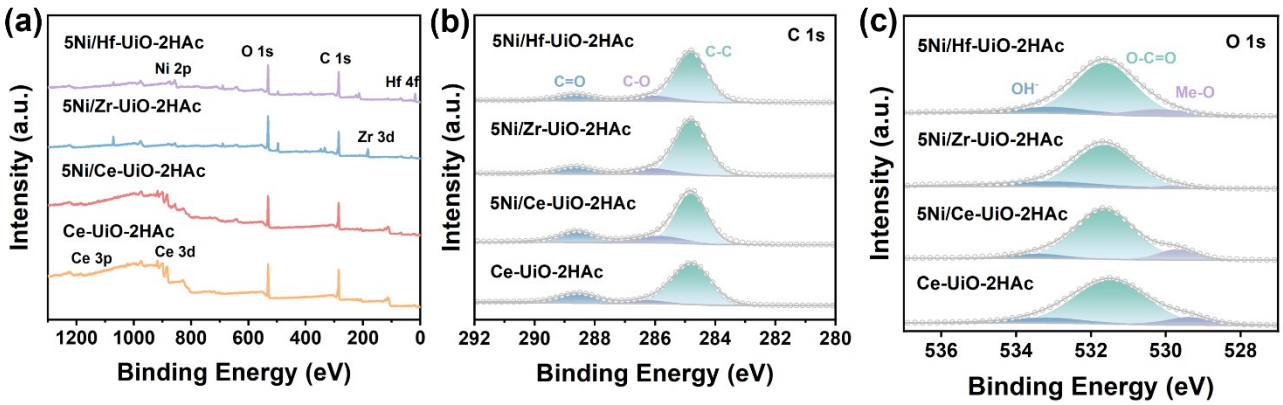

Figure S14. (a) XPS survey, XPS spectra of (b) C 1s and (c) O 1s from Ce-UiO-2HAc, 5Ni/Ce-UiO-2HAc, 5Ni/Zr-UiO-2HAc and 5Ni/Hf-UiO-2HAc.

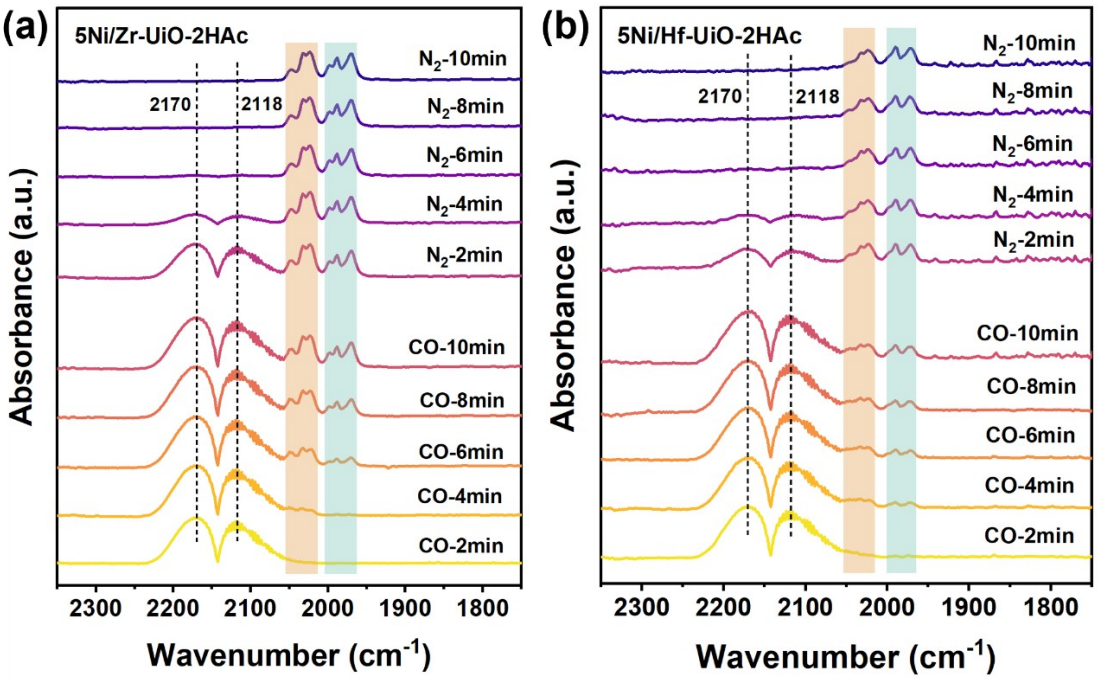

Figure S15. CO-DRIFTS of (a) 5Ni/Zr-UiO-2HAc, (b) 5Ni/Hf-UiO-2HAc.

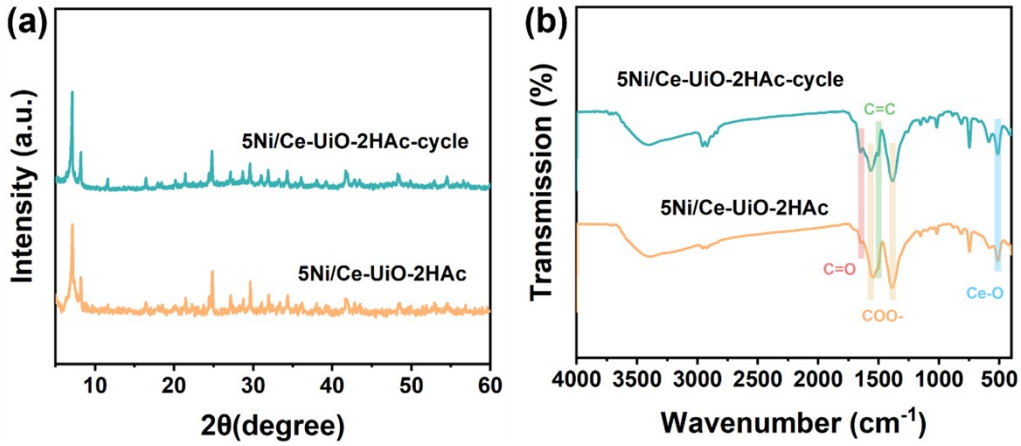

Figure S16. (a) XRD patterns, (b) FTIR spectra of 5Ni/Ce-UiO-2HAc and 5Ni/Ce-UiO-2HAc-cycle.

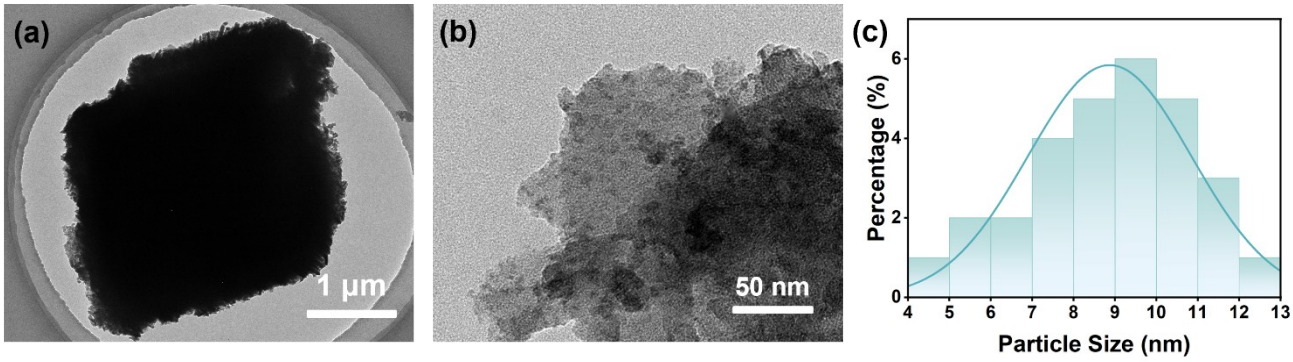

Figure S17. (a) and (b) TEM images, (c) Ni NPs size distribution of 5Ni/Ce-UiO-2HAc-cycle.

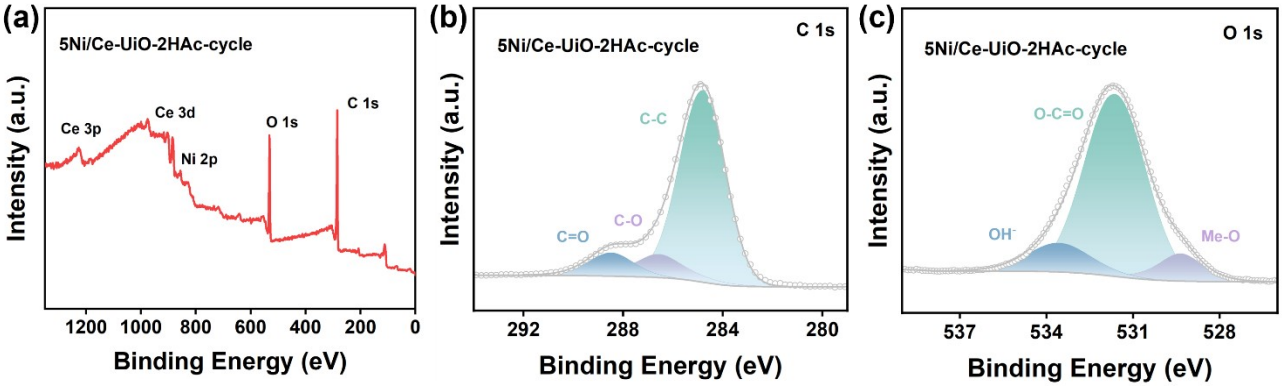

Figure S18. (a) XPS survey, XPS spectra of (b) C 1s and (c) O 1s from 5Ni/Ce-UiO-2HAc-cycle.

Table S1. Summary of the TG properties of catalysts.

Catalysts	ΔW (%)	W_{End} (%)	Coordination number of each Ce_6	Linker deficiency number of each Ce_6
Ce-UiO-1HAc	35.9	54.0	4.63	1.37
Ce-UiO-2HAc	33.6	54.6	4.31	1.69
Ce-UiO-3HAc	33.7	54.1	4.34	1.66
Ce-UiO-4HAc	32.7	52.9	4.31	1.69
Ce-UiO-5HAc	33.2	52.9	4.37	1.63

Table S2. ICP-MS data of catalysts.

Catalysts	Theoretical loadings (wt%)	Experimental loadings (wt%)
5Ni/Ce-UiO	5	4.965
1Ni/Ce-UiO-2HAc	1	0.754
3Ni/Ce-UiO-2HAc	3	2.710
5Ni/Ce-UiO-2HAc	5	5.104
7Ni/Ce-UiO-2HAc	7	6.898
5Ni/Zr-UiO-2HAc	5	5.168
5Ni/Hf-UiO-2HAc	5	4.793
5Ni/Ce-UiO-2HAc-cycle	5	4.624

Table S3. Pore features of catalysts from Nitrogen sorption isotherms.

Catalysts	S_{BET} (m^2/g)	V_{total} (cm^3/g)	S_{meso} (m^2/g)	V_{meso} (cm^3/g)	S_{micro} (m^2/g)	V_{micro} (cm^3/g)
Ce-UiO	1152.674	0.632	/	/	1152.674	0.632
Ce-UiO-1HAc	944.858	0.824	143.385	0.307	801.473	0.517
Ce-UiO-2HAc	623.280	0.572	316.289	0.431	306.991	0.141
Ce-UiO-3HAc	300.762	0.549	245.120	0.422	55.642	0.127
Ce-UiO-4HAc	289.630	0.596	222.373	0.540	67.257	0.056
Ce-UiO-5HAc	90.479	0.367	76.388	0.343	14.091	0.024
1Ni/Ce-UiO-2HAc	613.647	0.571	286.541	0.465	327.106	0.106
3Ni/Ce-UiO-2HAc	581.614	0.510	256.302	0.340	325.312	0.170
5Ni/Ce-UiO-2HAc	568.688	0.506	245.570	0.374	323.118	0.132
7Ni/Ce-UiO-2HAc	567.158	0.517	246.384	0.419	320.774	0.098
Zr-UiO-2HAc	922.513	0.701	219.642	0.216	702.871	0.485
Hf-UiO-2HAc	720.119	0.465	155.436	0.176	564.683	0.289

Table S4. The peak-area ratios of Ce 3d and Ni 2p were quantitatively analyzed by XPS.

Catalysts	Ce^{3+}/Ce^{4+}	Ni^{0}/Ni^{2+}
Ce-UiO-2HAc	0.48	/
5Ni/Ce-UiO-2HAc	0.61	0.27
5Ni/Zr-UiO-2HAc	/	0.17
5Ni/Hf-UiO-2HAc	/	0.18
5Ni/Ce-UiO-2HAc-cycle	0.55	0.25

Table S5. Summary reports of catalysts by H_2-TPD.

Catalysts	High-Temperature region		Low-Temperature region	
	High Temperature at Maximum (℃)	Quantity (mmol/g)	Low Temperature at Maximum (℃)	Quantity (10^{-2}mmol/g)
1Ni/Ce-UiO-2HAc	189.3	0.239	76.1	6.172
3Ni/Ce-UiO-2HAc	190.4	0.244	81.5	5.238
5Ni/Ce-UiO-2HAc	188.2	0.282	84.8	5.902
7Ni/Ce-UiO-2HAc	189.4	0.230	86.4	4.011